Probabilistic Capacity of Structural Insulated Panel and Its Use for Calibrating Codified Design

S.C. Yang
Assoc. Professor, Highway College, Chang'an University, Xi'an, China.

Y.H.Chui
Professor, Department of Civil & Environmental Engineering and the School of Mining & Petroleum Engineering, University of Alberta, Edmonton, Alberta, Canada.

H. P. Hong
Professor, Department of Civil and Environmental Engineering, University of Western Ontario, London, Ontario, Canada.

ABSTRACT: In the present study, we first report the experimental studies focused on the investigation of the behavior of a structural insulated panel (SIP) subjected to various load cases. The experimental results are then used as the basis to develop and implement finite element (FE) models that can be used to predict the response of SIP to compression, bending, and racking loads. Uncertainty propagation analysis is carried out using developed FE models and considering the uncertainty in material properties to provide a probabilistic characterization of the capacity of the SIP-spline wall/floor system. Finally, a probability distribution fitting exercise was carried out to identify the preferred probability distribution for the ultimate capacity of the SIP shearwall subjected to racking load, the SIP assembly subjected to out-of-plane bending in the major direction, and the SIP shearwall subjected to compression. The fitting and statistical criterion indicates that lognormal distribution, Weibull distribution, and Gumbel distribution are preferred for the ultimate capacity of the SIP-spline wall/floor subjected to racking, bending and compression loads, respectively.

1. INTRODUCTION

A structural insulated panel (SIP) is a composite wood-based material typically consisting of two sheets of oriented strand board (OSB) and a sandwiched lightweight foam core. The face OSB sheets are designed to resist axial and flexural stresses while the foam core with sliding-resistant adhesive improves shear capacity and buckling performance. SIPs can be used for the building envelope. SIPs are connected in the same plane by the lumber splines at the edges to form a stiff and energy efficient panel-frame wall system.

SIP is an industrialized material but the detailed design methodologies or properties for SIP, or SIP-spline wall/floor system, are not available in the wood design code in Canada (CSA 2019). Design methodologies for SIP should take into account the uncertainty in the material properties and structural response characteristics of SIP. Experimental studies have been carried out to investigate the behavior of SIP subjected to various load cases. It has been observed that SIPs subjected to concentric and eccentric axial loads have an approximately linear-brittle failure mode (Kermani and Hairstans 2006; Mousa and Uddin 2012; Tejchman 2014; Jacques and Makar 2019b). Failure includes the shear failure of the foam core and the crushing, wrinkling (i.e., buckling), or debonding of the face sheet. The failures are mostly due to the stress concentration at the ends or the quarter height of the panel. These experimental studies were focused on the SIP itself, and the investigation of the behavior of a panel-frame wall system formed by the SIPs was lacking. Moreover, the tested SIPs are generally hinged at the top and bottom,

that is, no relative deformation between SIPs and the connected splines is considered. Therefore, the assessed compressive stiffness of SIP from the observed failure modes could be unconservative since the effect of the inelastic deformation of the connections between SIPs and the splines was ignored. Moreover, the failure due to the crushing of the horizontal splines may be the predominant failure mode that could lead to a lower design compressive resistance of SIP as compared to that obtained from the mentioned studies.

Jacques and Makar (2019a, b) developed a design expression for predicting the strength of full-size panels subjected to out-of-plane transverse loads or axial loads, and the developed expression was further calibrated through reliability analyses but the uncertainties of the capacity of SIP was not considered in their studies. The probabilistic characterization of the capacity of SIP requires a number of tests associated with too many test variables and mixed-mode failure conditions. To reduce the effort of testing and simplify the research procedures, a numerical simulation of SIP was employed by Foschi (2006). The numerical results were used to assess the response surface and the failure probability of SIP due to compression, bending, or racking load. Numerical models have also been developed by Mousa and Uddin (2012) and Tejchman (2014) and the results are compared to the test results. However, the models were focused on the SIP without splines, and the influence of the splines and inelastic connections on the structural behavior was ignored.

The objectives of the present study were to 1) develop finite element (FE) models for predicting the response of SIP to compression, bending, and racking loads, 2) validate the developed FE model using the experimental test results, and 3) carry out uncertainty propagation analysis using the developed FE models and considering the uncertainty in material properties to provide a probabilistic characterization of the capacity of SIP-spline wall/floor system.

2. FINITE ELEMENT MODELLING OF SIP

2.1. General consideration

A proprietary SIP constructed using oriented strand board (OSB), polyisocyanurate foam, and lumber was considered in the following. The panel is shown in Figure 1a. The spline members between panels, top and bottom wall plates are No. 2 and better grade Spruce-Pine-Fir (SPF) dimension lumber with design properties specified in CSA O86-14 (2014). The OSB is 11 mm in thickness. The core polyisocyanurate foam is either 89 or 140 mm in thickness and the intermediate foam layer (i.e., thermal break), if present, is 12.5 mm in thickness.

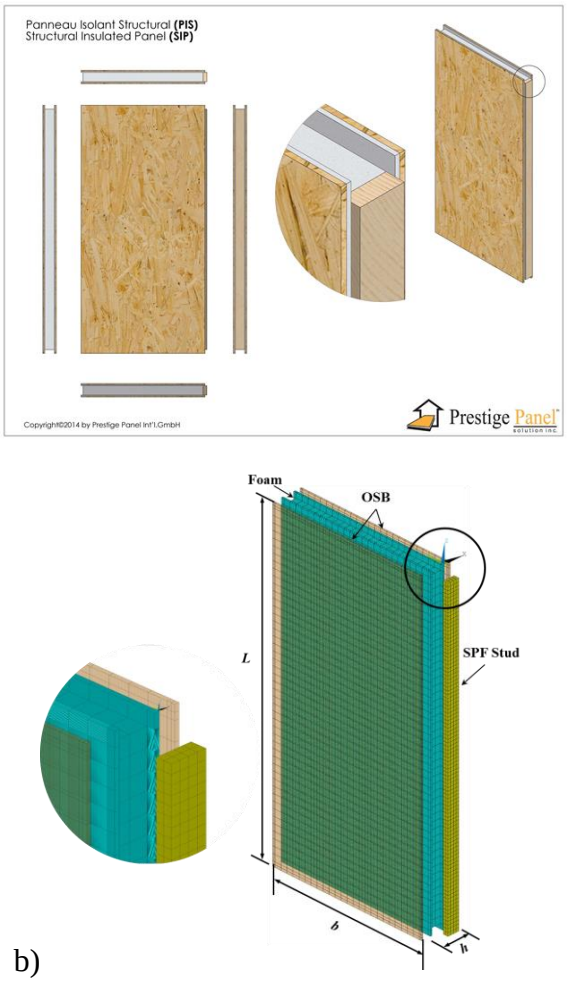

Figure 1: *Illustration of the SIP and corresponding finite element model: a) Illustration (WSTC 2014); (b) 3D FE model.*

The 3D FE models of SIP were developed in ANSYS (2016) by considering five

configurations of SIPs. The developed models subjected to racking, bending, and compression are illustrated in Figure 1b, where the symbols *L*, *b*, and *h* used to define the dimensions are also illustrated in the figure. Values of *L*, *b*, and *h* for the considered SIP configurations are given in Table 1. The corresponding developed FE models are also shown in the same figure.

Table 1. Identification (ID) of considered SIP configurations.

ID	*L* (mm)	*b* (mm)	*h* (mm)	Thermal break	Longitudinal spline
1	2440	1220	136	With thermal break (WTB)	2×4 SPF
2	2440	1220	111	No thermal break (NTB)	2×4 SPF
3	2440	1220	187	With thermal break (WTB)	2×6 SPF
4	2440	1220	162	No thermal break (NTB)	2×6 SPF
5	2740	1220	136	With thermal break (WTB)	2×4 SPF

For developing the FE models of SIP, the OSB, lumber, and foam components of the SIP were modelled using SOLID185 (eight nodes) elements. These components were meshed with a size of 50 mm, except for the critical regions that are likely to experience concentrated stress. For these regions, a refined element size as illustrated in Figure 1b was used. The OSB, lumber, and foam are orthotropic with the material properties shown in Table 2.

For the modeling, the OSB and foam were assumed to be fully glued (i.e., no slippages occur). A similar modelling approach was taken for the interaction between the top plate and cap, and between the bottom plates. The contact behavior between longitudinal splines to other components was modeled by a hard contact model normal to the contact surface, that the compression between the adjacent elements was coupled whereas the tension is not transferred, and it was assumed to be frictionless. This consideration facilitates the modeling of the nail joint connections. The modelling of behaviour of SIP under various loading cases, such as the constitutive models, is described in the following sections.

Table 2. Material properties.

Property		OSB(2)	Foam(3)	Lumber(4)
Elastic modulus (MPa)	E_x(1)	4265	9.541	9600
	E_y or E_z	3445	7.082	965
Shear modulus (MPa)	G_{xy}	650	2.693	1296
	G_{yz} or G_{xz}	640	2.252	900
Poisson's ratios	ν_{xy}	0.23	0.25	0.4
	ν_{xy} or ν_{xy}	0.16	0.25	0.4
Compressive strength (MPa)	f_c	14.8	0.17	28.2
	f_{cp}	12.8	0.15	5.3
Tensile strength (MPa)	f_t	11.8	-	23.3

Note: (1). Subscript *x* represents the major direction of the material; subscripts *y* and *z* represent the minor directions of the wood materials. (2). The material properties for the OSB are from manufacturers, except that the Poisson's ratios for OSB are from Thomas (2003). (3). The material properties of the polyurethane foam are the mean values of the test results. (4). Values for SPF lumber are based on the following considerations: (a). E_x, G_{xy}, f_c, and f_t are adopted from the Canadian Lumber Properties (Barrett and Lau 1994). The mean values from the test data are used; (b). E_y or E_z, G_{yz} or G_{xz}, and the Poisson's ratios for SPF are adopted from Green et al. (1999); (c). f_{cp} is calculated according to CSA O86-14 (2014) with G equal to 0.42.

2.2. Modelling of SIP subjected to different loading

Since a ready-to-use model with calibrated parameters for the nail joints for the considered system in the present project is unavailable, a fitting approach was employed to calibrate the model parameters of the nail joints such that the predicted responses are in agreement with the experimental tests.

The nail joint was modelled using the 2-node COMBIN39 spring element with defined loading and unloading paths. The element was capable of simulating the elastic, yielding, hardening, and damage evolution of the nail joint. The element has one translational degree of freedom at each node (see Figure 2). The force-deformation

relation of the spring element was determined by a set of deformation and force (D_i, F_i) values.

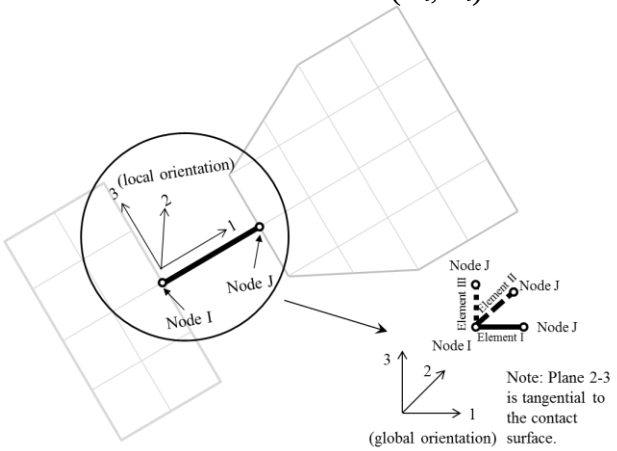

Figure 2: *Modelling of the nail joint.*

Although the analysis and comparison for the five configurations shown in Table 1 were carried out, only a typical fitted force-deformation relation for WTB is illustrated in Figure 3a.

The tests of SIP shearwall subjected to racking load (i.e., in-plane lateral loads) were carried out and a FE method was developed. The analysis indicates that the developed FE model with calibrated model parameters can adequately represent the test results, as illustrated in Figure 3b. Tests of SIP shearwall subjected to bending in the major direction were carried out and a FE model was developed. An example comparison of the analysis results obtained by using the developed FE model with calibrated model parameters to the test results is presented in Figure 3c, indicating that they are in good agreement.

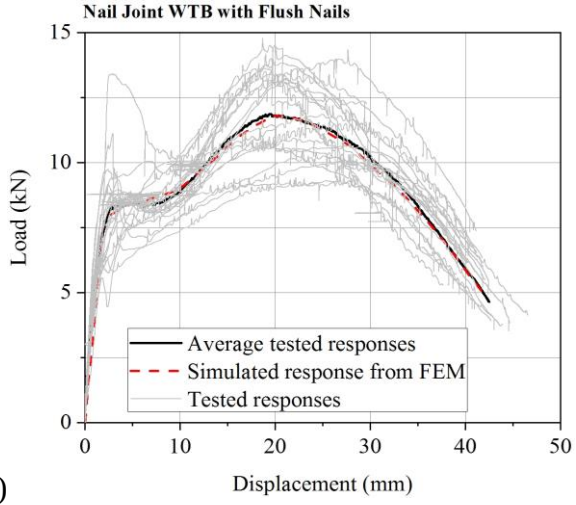

a)

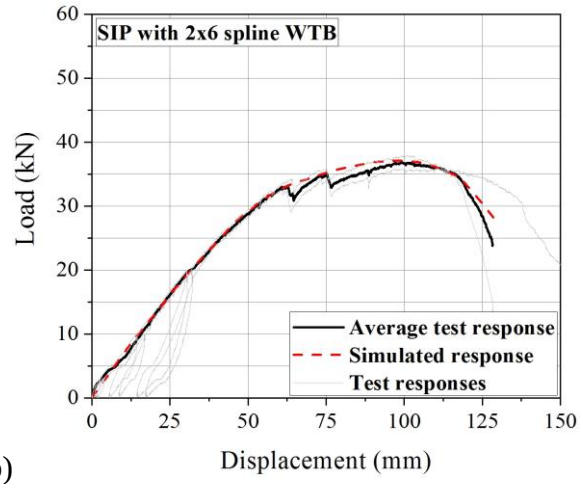

b)

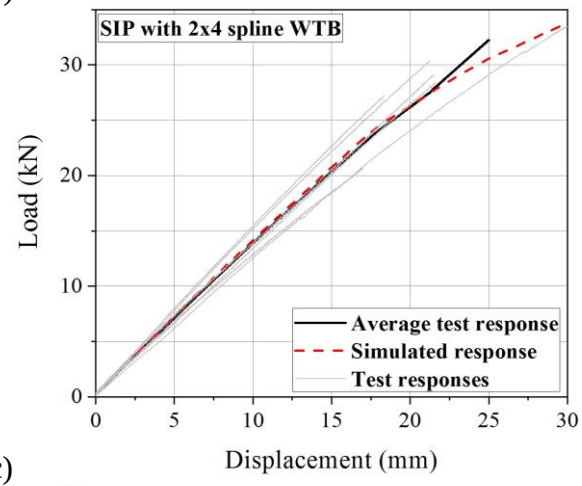

c)

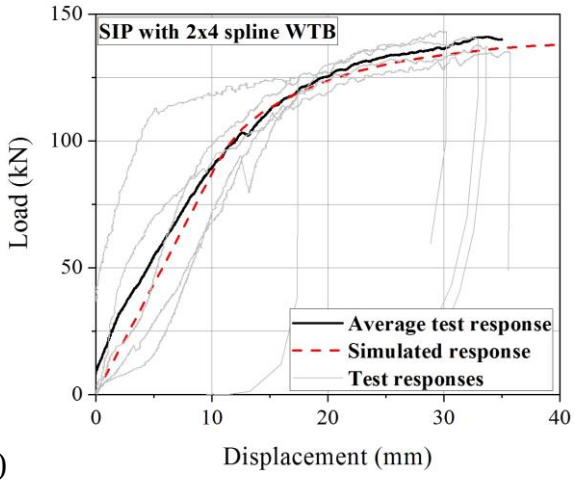

d)

Figure 3. Results based on the developed FE models and test results for WTB. a) force-deformation for nail joint (racking load); b) Load-displacement curves of SIP shearwall subjected to racking load; c) force-displacement curve of SIP assembly subjected to bending in the major direction; d) Load-displacement curves of SIP shearwall subjected to compression.

In addition, tests of SIP subjected to eccentric compression were carried out and a FE model for such a loading case was developed. An example comparison of the analysis results obtained by using the developed FE model with calibrated model parameters to the test results is presented in Figure 3d, indicating that they are in good agreement.

3. PROBABILISTIC CHARACTERIZATION OF THE CAPACITY OF SIP

For the probabilistic assessment of the capacity of the SIP, the developed FE models were employed for SIP subjected to the racking load;, the developed FE models that were modified for SIP subjected to bending or compression load were also considered. For the case that SIP was subjected to bending, the model was modified according to the code specified dimensions (e.g., width×height is 1220 mm×2400 mm) by removing the elements representing half of the spine at each longitudinal edge. Such a modification is aimed at providing the capacity and limit state information that could be useful for evaluating the reliability-based design considered by the design code (CSA 2019).

For the probabilistic assessment of the capacity of SIP, the considered basic random variables are shown in Table 3. In the table, the probabilistic models for the material properties (except those for SPF) were obtained by assessing the test data from a preliminary experimental study on OSB. The probabilistic characterization for these material properties was performed and the fitted distribution types are also given in Table 2. Considering that the sample size was relatively small due to the limited number of specimens, the probabilistic model is assigned according to Foschi (2006) if the most preferable distribution was not available. The uncertainties considered for the material properties (except for the compressive strength of SPF perpendicular to the grain) of SPF in grade No. 2 were adopted from Barrett and Lau (1994).

Using the developed FE models and considering the probabilistic models of the random variables shown in Table 3, the probabilistic assessment of the capacity of the SIP was carried out using the Latin hypercube sampling technique (Rubinstein and Kroese 2016; Melchers and Beck 2018). For each resistance (i.e., ultimate capacity) of interest, 500 samples of the capacity curve were evaluated.

Typical samples of capacity curves were shown in Figure 4 by considering the SIP shearwall subjected to racking load. For each plot in Figure 4, only 100 samples rather than 500 samples were used to reduce the clutter. Also, the ultimate capacity and the mean capacity curve are identified in the figure. As can be observed in Figure 4, there is a significant scatter in the ultimate capacity of SIP subjected to racking load. Similar analyses were carried out by considering SIPs subjected to bending in the major direction, and SIP shearwall subjected to axial compression. However, the results are not presented here to save space.

To provide a probabilistic characterization of the ultimate capacity of SIP, 500 samples of the ultimate capacity for each SIP configuration and each loading scenario were considered. For the SIP configurations described in Table 1, the samples are presented in the lognormal paper in Figure 5 by considering the SIP shearwall subjected to racking load. The results shown in Figure 5 indicates that the lognormal distribution may be considered adequate for such ultimate capacity since the empirical distribution follows approximately a straight line. To further identify the preferred probability distribution, a fitting exercise was carried out for the ultimate capacity by using the commonly used distributions such as normal, lognormal, Weibull, and Gumbel distributions (Benjamin and Cornell 2014). Based on visual inspection as well as the use of Akaike information criterion (AIC), the lognormal distribution was preferred among the considered distribution models.

Table 3. Statistics of the random variables considered for SIP (the unit for stress related properties is MPa, and the unit of dimension is mm).

No.	Random variable	Mean	CoV	Distribution type
1	E_x of OSB[(1)(2)(3)]	4265	0.213	Weibull
2	E_y and E_z of OSB	3445	0.292	Weibull
3	G_{xy} of OSB	650	0.172	Weibull
4	G_{yz} and G_{xz} of OSB	640	0.147	Weibull
5	E_x of foam	9541	0.254	Lognormal
6	E_y and E_z of foam	7082	0.241	Lognormal
7	G_{xy} of foam	2693	0.259	Lognormal
8	G_{yz} and G_{xz} of foam	2252	0.255	Lognormal
9	E_x of SPF	9665	0.098	Normal
10	E_y and E_z of SPF	965	0.150	Normal
11	G_{xy} of SPF	1296	0.150	Normal
12	G_{yz} and G_{xz} of SPF	900	0.150	Normal
13	Compressive strength of OSB parallel to grain	14.8	0.177	Weibull
14	Compressive strength of OSB perpendicular to grain	12.8	0.192	Weibull
15	Tensile strength of OSB parallel to grain	11.8	0.215	Lognormal
16	Tensile strength of OSB perpendicular to grain	8.5	0.208	Lognormal
17	Compressive strength of foam	0.16	0.178	Gumbel
18	Compressive strength of SPF parallel to grain	28.2	0.190	Weibull
19	Compressive strength of SPF perpendicular to grain[(4)]	5.3	0.190	Weibull
20	Tensile strength of SPF parallel to grain	23.3	0.250	Weibull
21	t_c, top OSB thickness	11	0.032	Normal
22	t_t, bottom OSB thickness	11	0.032	Normal
23	b, panel width[(5)]	1220	0.034	Normal
24	L, panel length[(5)]	2440	0.034	Normal
25	Nail joints stiffness	[(6)]	0.230	Lognormal

Note: (1). E and G are the elastic modulus and shear modulus, respectively. The subscript x represents the major direction (i.e., parallel to grain); (2). The material properties are applied to the members made from the same material. For example, the same elastic modulus of OSB is used for the top and bottom OSB, and the same material properties are used for each SPF spline; (3). The statistics for the material properties of OSB are obtained from the results of the tests conducted on the products from five manufacturers. The probabilistic models are in accordance with Foschi (2006); (4). The statistic for compressive strength of SPF perpendicular to the grain is not available in the literature. The assumed probabilistic model is given in the table; (5). The panel width governs the width of OSB and foam core, and the panel length governs the length of OSB, foam core, and SPF studs; (6). The stiffness of nail joints is determined by a set of parameters in the FE model, they are scaled by the same factor for the simulation.

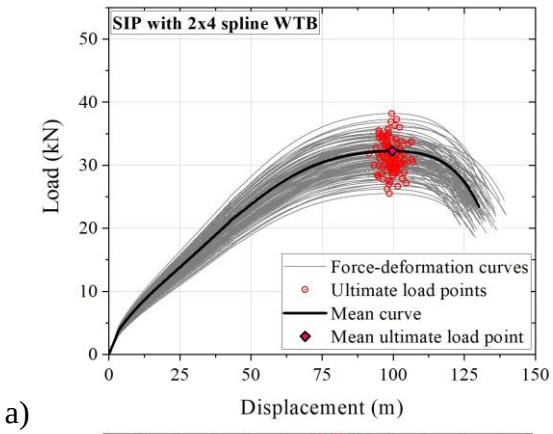

a)

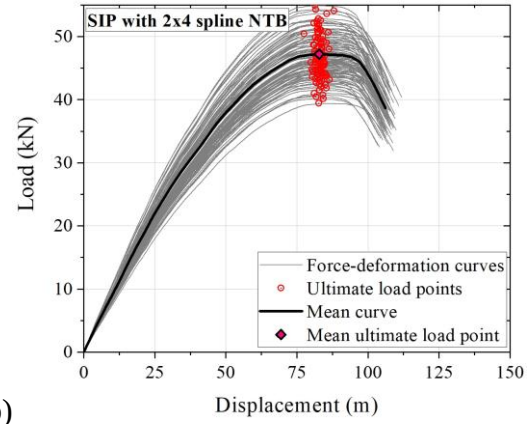

b)

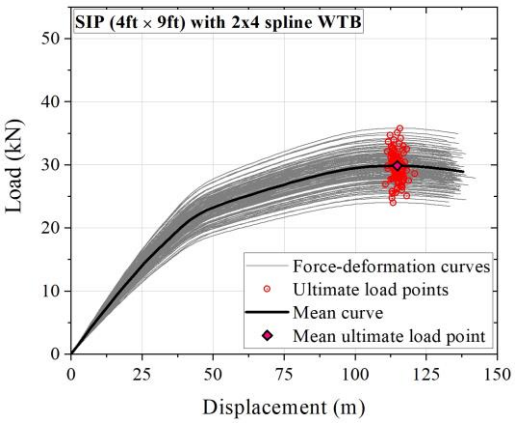

c)

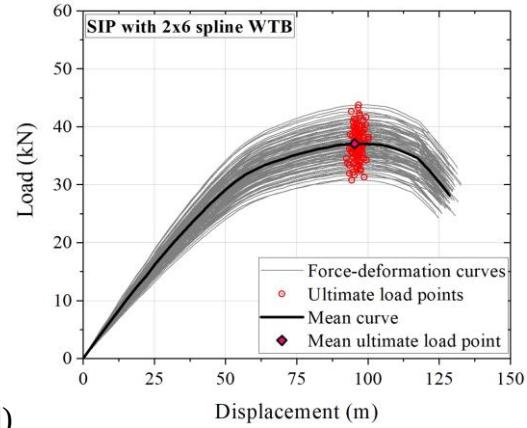

d)

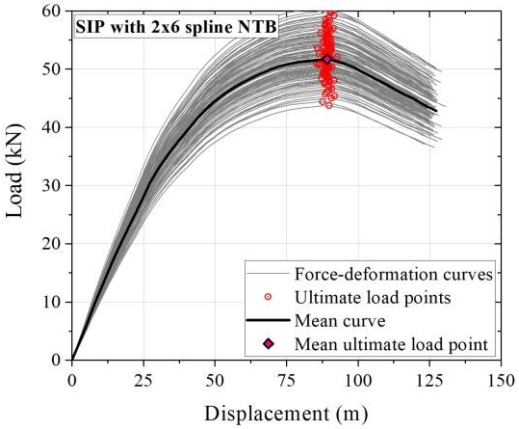

e)

Figure 4. Capacity curve obtained based on developed FE models and simulation analysis. of SIP considering racking load: a) -e) are plots by considering different SIP configurations.

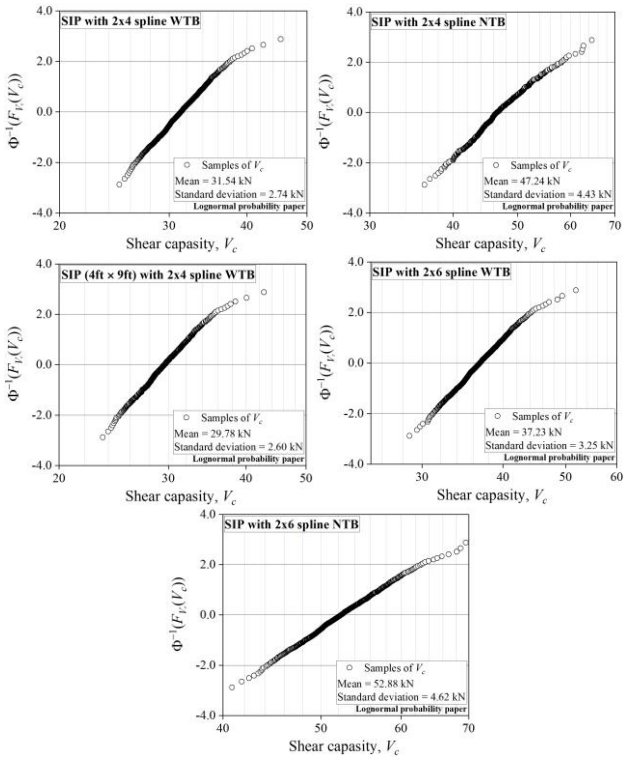

Figure 5. Empirical distribution of ultimate capacity of different configrations of SIP shearwall subjected to racking load.

Similar analysis was carried out by considering the SIP assembly subjected to bending in the major direction, and the SIP shearwall subjected to axial compression. The obtained results (which are not shown in here due to space limitation) indicated that the Weibull

distribution is preferred for the ultimate capacity of SIP subjected to bending and the Gumbel distribution is preferred for the ultimate capacity of SIP subjected to axial compression.

4. CONCLUSIONS

The SIP-spline wall/floor system with five configurations was analysed by using the finite element method for assessing the probabilistic characteristics of their capacity considering different load cases. The finite element models for the considered load cases were developed by adopting the properties of each component of SIP obtained from a test program. The comparison between the obtained responses from the simulation and the test program indicates that the finite element models can predict the responses adequately, at least on average.

The probabilistic characterization for the capacity of SIP was carried out considering the material uncertainties assessed from the test results or from the literature. It indicated that the lognormal distribution, Weibull distribution, and Gumbel distribution are preferred for the ultimate capacity of the SIP-spline wall/floor subjected to racking, bending and compression loads, respectively. In addition, the deflections of SIP shearwall under racking loads were probabilistically fitted, showing that the deflection is distributed lognormally. For the vertical displacements of SIP-spline walls under compression, it was found that the vertical displacement is also a lognormal random variable when the end eccentricity is less than or equal to 1/6 of the thickness of SIP. It was also found that the effect of end eccentricity is not significant on the vertical displacement of the SIP-spline wall for the load level considering the serviceability limit state. The probabilistic characteristics of the capacity of SIP are presented. The information can be used for further employment of the reliability assessment, which is critical for investigating the design methodologies or properties of SIP.

5. REFERENCES

Barrett, D. L., & Lau, W. (1994). Canadian lumber properties. Canadian Wood Council, Ottawa, ON.

Benjamin, J. R., & Cornell, C. A. (2014). Probability, statistics, and decision for civil engineers. Courier Corporation.

Canadian Standards Association. (2019). 'Engineering design in wood'. CSA O86-19.

Foschi. (2006). PANEL: a general structural analysis for stressed-skin panels and SIP: a performance/reliability-based design for structural insulated panels. Report. Prepared for Plasti-Fab, Division of PFB Corporation.

Green, D. W., Winandy, J. E., & Kretschmann, D. E. (1999). Mechanical properties of wood. Wood handbook: wood as an engineering material. Forest Products Laboratory.

Jacques, E., & Makar, J. (2019a). Behavior of Structural Insulated Panels Subjected to Short-Term Axial Loads. *Journal of Structural Engineering*, *145*(11), 04019118.

Jacques, E., & Makar, J. (2019b). Behaviour of structural insulated panels (SIPs) subjected to short-term out-of-plane transverse loads. *Canadian Journal of Civil Engineering*, *46*(9), 858-869.

Kermani, A., & Hairstans, R. (2006). Racking performance of structural insulated panels. *Journal of structural Engineering*, *132*(11), 1806-1812.

Melchers, R. E., & Beck, A. T. (2018). Structural reliability analysis and prediction. John wiley & sons.

Mousa, M. A., & Uddin, N. (2012). Structural behavior and modeling of full-scale composite structural insulated wall panels. *Engineering Structures*, *41*, 320-334.

Rubinstein, R. Y., & Kroese, D. P. (2016). Simulation and the Monte Carlo method. John Wiley & Sons.

Tejchman, J. (2014). Evaluation of strength, deformability and failure mode of composite structural insulated panels. Materials & Design (1980-2015), 54, 1068-1082.

Thomas, W. H. (2003). Poisson's ratios of an oriented strand board. Wood science and technology, 37(3-4), 259-268.

WSTC. (2014). Evaluation of structural insulated panels manufactured by prestige panel solution Inc.. Report reference # WSTC2014-018. Wood Science and Technology Center.